Realization of Polymeric Optical Integrated Devices Utilizing Organic Light-Emitting Diodes and Photodetectors Fabricated on a Polymeric Waveguide

Yutaka Ohmori, *Senior Member, IEEE*, Hirotake Kajii, Masamitsu Kaneko, Katsumi Yoshino, *Fellow, IEEE*, Masanori Ozaki, Akihiko Fujii, Makoto Hikita, Hisataka Takenaka, and Takayuki Taneda

***Abstract*—Direct fabrication of organic light-emitting diodes (OLEDs) and organic photodetectors (OPDs) on polymeric substrates, i.e., polymeric waveguide substrates to form flexile optical integrated devices is demonstrated. The OELD and OPD were fabricated by organic molecular beam deposition (OMBD) technique on a polymeric or a glass substrate, for comparison. The device fabricated on a polymeric substrate shows similar device characteristics to that on a glass substrate. Optical signals of faster than 100 MHz have been created by applying pulsed voltage directly to the OLED utilizing diamine derivative, or rubrene or porphine doped in 8-hydoxyquinolinum aluminum derivatives, as an emissive layer. Electrical signals are successively converted to optical signals for optical transmission of moving picture signals with OLED fabricated on a polymeric waveguide. OPDs utilizing phthalocyanines derivatives with superlattice structure provide increased pulse response with input optical signals, and the OPD with the cutoff frequency of more than 5 MHz has been realized.**

***Index Terms*—Optical integrated circuits, organic light-emitting device, organic photodetectors, polymeric waveguide.**

I. Introduction

ORGANIC light-emitting diodes (OLEDs) [1] utilizing fluorescent dye or conducting polymer have attracted great interest because they have advantages for thin-film flat-panel display. An additional advantage is that they are simple for fabrication on various kinds of substrates, including polymeric substrates. Metal phthalocyanines are well-known materials which show good stability, photo activity, and with high mobility. Among them, fluorinated phthalocyanine shows high-electron mobility and will be suitable for photo-absorption and carrier generation layers of organic photodetectors (OPD) with combination with metal phthalocyanines. Forrest *et al.* reported high-speed OPD utilizing organic materials [2]. On the other hand, polymeric waveguide devices have attracted great attention with regard to their use for optical interconnection with high-speed transmission and flexible optical circuits. The combination of polymeric waveguide [3], OLED, and OPD will realize a flexible optical integrated devices [4], [5].

In this paper, we discuss the characteristics of OLEDs fabricated on polymeric substrates, i.e., polymeric waveguides and their application for optical transmission experiments. We also discuss photo response of OPDs, which consist of multilayered phthalocyanine derivatives and/or organic dye thin films.

II. Experimental

OLED with various emissive materials including red, yellow, green, and blue light emission have been investigated. The organic layers for OLEDs and OPD were vacuum deposited by organic molecular beam deposition (OMBD) at a background pressure of 10^{-5}Pa. For substrates used for the experiments polymeric substrates were used, however, glass substrates were also used as comparison. Polymeric waveguides were used as substrates, however, polyimide films were also employed as polymeric substrates, because they have high-thermal stability, high-optical transparency, and they are one of promising candidates for optical devices such as polymeric optical waveguide devices.

The output light from the OLED was introduced perpendicular to the substrate, using 45° cut mirror. That is, one of the edges of the polymeric waveguide was cut in 45°, which serves as a mirror, in order to introduce the optical output from the OLED to the waveguide. For a polymeric waveguide [3], deuterated-polymethylmethacrylate (d-PMMA) and ultraviolet (UV)-cured epoxy resin for core and the cladding of the polymeric waveguide, respectively, were used. The polymeric waveguide has a square core size of 70 μm. A graded-index multimode silica optical fiber with the core size of 200 μm and the length of 100 m was used for transmission experiments.

Schematic of polymeric optical integrated device fabricated on a polymeric waveguide is shown in Fig. 1. Here, OLEDs are used as electrooptic conversion devices and OPDs are used as opto-electric conversion devices. Polymeric waveguide is connected with an optical fiber with optical connectors. Electrical video or audio signals are converted with organic electroluminescence (EL) device to optical signal, and are transmitted to optical fiber through polymeric waveguide. And then, the optical signals are received to OPDs through the polymeric waveguide. The converted output signals of photodetectors are displayed on terminals such as displays, facsimiles, or phones.

Manuscript received April 18, 2003; revised August 5, 2003. This work was supported in part by the Ministry of Education, Culture, Sports, Science and Technology (MEXT) under a Grant-in-Aid for the Development of Innovative Technology under Project 12101, and in part by a Grant-in-Aid for Scientific Research in the priority area under Grant 13022241.

Y. Ohmori, H. Kajii, M. Kaneko, and T. Taneda are with the Collaborative Research Center for Advanced Science and Technology (CRCAST), Osaka University, Osaka 565-0871, Japan (e-mail: ohmori@crcast.osaka-u.ac.jp).

K. Yoshino, M. Ozaki, and A. Fujii are with the Department of Electronic Engineering, Osaka University, Osaka 565-0871, Japan.

M. Hikita and H. Takenaka are with the NTT Advanced Technology Corporation, Ibaraki 319-1193, Japan.

Digital Object Identifier 10.1109/JSTQE.2004.824106

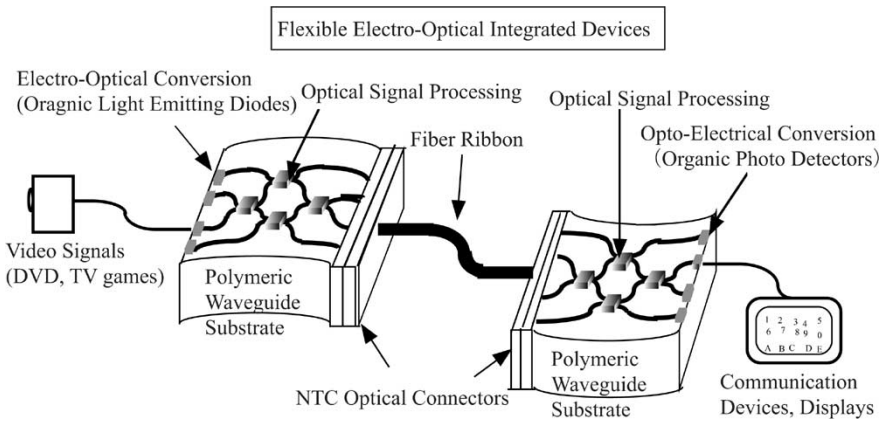

Fig. 1. Schematic of a polymeric optical integrated device.

The application of the proposed polymeric integrated devices will be used for local area network (LAN) for home use or for short-distance interconnections. For the use of the polymeric waveguide and organic devices, i.e., OLED and OPD, the transmission speed will be in the range of several hundreds megahertz.

In Fig. 2, schematic of the OLED and OPD are shown. A typical OLED, which is shown in Fig. 2(a), consists of indium-tin-oxide coated polymeric substrate with buffer layers with thin layers of silicone oxide and silicone nitride multilayers, hole transporting layer of 4, $4'$-bis[N-(1-napthyl)-N-phenyl-amino]-biphenyl (α-NPD), emissive layer (doped type or undoped type), electron transporting layer of 8-hydroxquinoline aluminum (Alq_3), terminated with cathode of silver-containing magnesium (Mg:Ag). As a dopant of the emissive layer, 5,6,11,12-tetraphenyl-naphthacene (rubrene) or 5,10,15,20 tetraphenyl-21H,23H-porphine (TPP) molecule was doped in Alq_3, respectively. In order to reduce the straight capacitance of the diode, the active size of the device were employed as small as 0.01 mm^2 and others. After deposition of the organic layers and the metal electrode, the OLEDs are sealed in an inert gas (Ar gas).

The OPDs were fabricated by OMBD technique similar to the OLED, whose typical device structure is shown in Fig. 2(b). The device consists of ITO transparent anode, photo absorbing, and carrier generation layers of alternating TiOPc and F_{16} MPc (M =Cu or Zn) layers or TiOPc and N, N'-bis(2,5-di-*tert*- butylphenyl)-3,4,9,10-perylenedicarboximimide (BPPC) layers, and a contact layer to the cathode of 2,9-dimethyl-4,7-diphenyl-1,10-phenanthroline (BCP).

As photo-absorbing layers in the OPD, superlattice structure of alternate layers of TiOPc and fluorinated phthalocyanine (F_{16}MPc, M =Zn or Cu), or TiOPc and BPPC were employed, and a number of the periods were chosen from a single heterostructure to ten periods of alternate layers. The total layer thickness with the superlattice structure for the photo-absorption layer was kept at the same value as 40 nm. The 20-nm-thick BCP layer inserted between the cathode and photo-absorption layers serves as a carrier blocking layer, and also prevents the photo-absorbing layer from the damage during metal deposition. After deposition of organic and metal

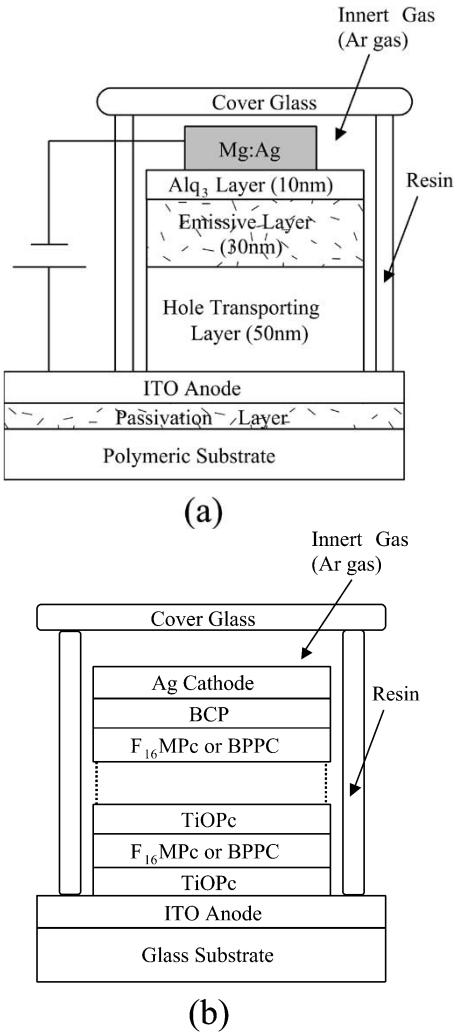

Fig. 2. Typical device structures. (a) OLED. (b) OPD.

electrode, the device was sealed in an inert Ar gas, similar to the OLED. The organic materials are shown in Fig. 3 together with those for OLED. The measurement of photo response has been performed with and without applied reverse bias to the organic photodetectors under an illumination of pulsed light of red LED (wavelength: 640 nm, output power: -6 dBm) through polymer optical fiber with 1 mm in core diameter.

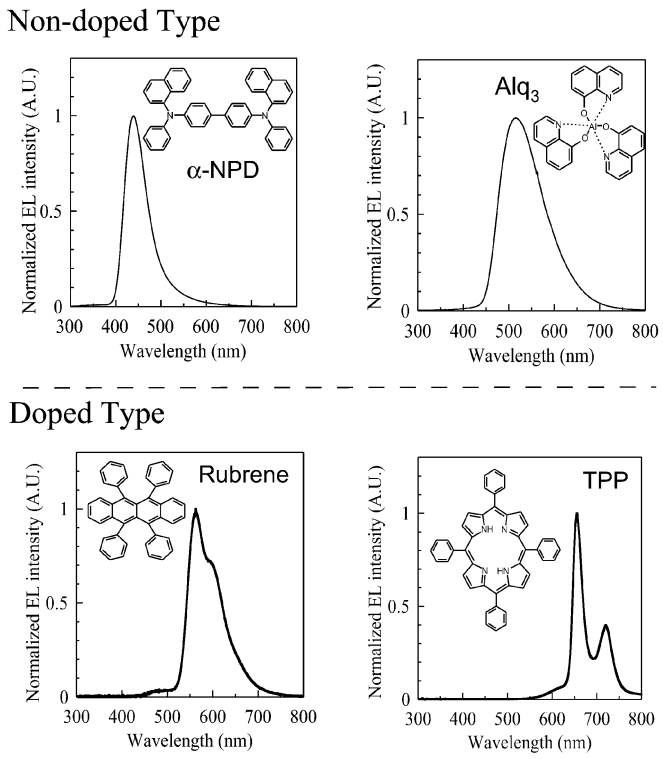

Fig. 3. Typical EL spectra of NPD, Alq3, rubrene, and porphine as emissive materials.

III. Results and Discussions for OLEDs

Some of the emission spectra of organic EL diodes are summarized in Fig. 3. The emission intensities are normalized as a unity. There are two types of organic materials for OLED; one for undoped type such as α-NPD and Alq_3, and the other is for doped type such as rubrene and porphine derivative (TPP), which are doped in a carrier transporting materials.

In case of a device in which α-NPD as an emissive layer, the device consists an ITO-coated glass substrate, 60-nm-thick α-NPD as a hole transporting and emissive layer, 5-nm-thick 4,4′-bis(carbazol-9-yl)-biphenyl (CBP), 10-nm-thick 2′,9-dimethy-4,7-diphenyl-1,10-phenanthroline (BCP) as hole-blocking layers, and 15-nm-thick (Alq_3) as an electron transporting layer, terminated with a silver containing magnesium (Mg:Ag) cathode. The device emits clear blue emission centered at about 435 nm, and the turn-on voltage of the device is about 3 V. The emission intensity reaches to 8 mW/cm^2 at an injection current density of 1 A/cm^2, and to 25 mW/cm^2 at 5 A/cm^2. It finally reaches to a maximum intensity of 40 mW/cm^2. The clear light pulses were created by direct modulation of the OLED with an active area of 0.01 mm^2 under the applied pulse of 100 MHz.

Second device is made with Alq_3 as an emissive material. The device consists an ITO-coated glass substrate, 50-nm-thick α-NPD as a hole transporting layer, 50-nm-thick Alq_3 as an emissive and electron transporting layer, terminated with a silver containing magnesium (Mg:Ag) cathode. The device emits clear green emission centered at about 520 nm. The emission reaches to 30 mW/cm^2 with an applied voltage of 10 V and at an injection current density of 6 A/cm^2. However, the modulation characteristics are rather poor compared with α-NPD device, and its high-frequency modulation limited to 60 MHz. It is difficult to obtain optical pulses of more than 60 MHz using the green emitting Alq_3 as an emissive material, because the fluorescence lifetime of Alq_3 is more than 10 ns.

TABLE I
Summary of Emission Characteristics of Various Kinds of OLEDs

Emissive Materials	α-NPD	Alq_3	Rubrene	TPP
Emission Wavelength	430nm	520nm	560nm	655nm 720nm
Emission Intensities (at 5 A/cm^2)	More than 25mW/cm^2	More than 30mW/cm^2	More than 30mW/cm^2	More than 3mW/cm^2
Frequency Limitation	More than 100MHz	60MHz	More than 100MHz	More than 100MHz

The third device consists of rubrene doped in Alq_3 layer as an emissive layer. In Fig. 3, shown is the emission spectra of OLED with 9.1 vol % of rubrene doped in Alq_3 layer. The device consists of 50-nm-thick α-NPD as a hole transporting layer, 30-nm-thick rubrene doped in Alq_3 as an emissive layer and 10-nm-thick Alq_3 as an electron transporting layer, terminated with a Mg:Ag cathode. The device emits clear yellow emission centered at about 560 nm. The emission reaches to 30 mW/cm^2 at a current density of 5 A/cm^2. The modulation characteristics will be discussed in later paragraph.

The emission spectrum of red light-emitting device is also shown in Fig. 3. The device consists of 50-nm-thick α-NPD as a hole transporting layer, 30-nm-thick TPP doped in Alq_3 as an emissive layer, 10-nm-thick BCP layer as a hole blocking layer, a 10-nm-thick Alq_3 layer as an electron transporting layer, and terminated with a Mg:Ag cathode. The mole fraction of TPP is only 1%, and it is sufficient for emitting red light. The emission spectra have two peaks centered at 650 nm and 720 nm. The modulation frequency reaches at 100 MHz as is similar to the device with α-NPD as an emissive layer. However, the emission intensity is rather poor compared with other materials due to the poor emission efficiency, and the maximum emission intensity is 3 mW/cm^2 at a current density of 5 A/cm^2. The emission characteristics of OLEDs are summarized in Table I with the pulse modulation characteristics.

In Fig. 4, emission characteristics are compared as a function of injection current for the OLED with 50-nm-thick Alq_3 as an emissive layer and 50-nm-thick α-NPD as a hole transport layer fabricated on a glass and polyimide substrate. The device emits clear green emission centered at about 520 nm. As shown in Fig. 5, the emission reaches 50 000 cd/m^2, at an applied voltage of 10 V and the current density of 5 A/cm^2. The emission intensity is equivalent to about 30 mW/cm^2. The emission characteristics of the OLED fabricated on a polymeric substrate shows similar characteristics to that on a glass substrate, however, the emission efficiency is rather high in the device with polymeric substrate. The emission reaches 50 000 cd/m^2, at an applied voltage of 10 V and the current density of 6 A/cm^2. The

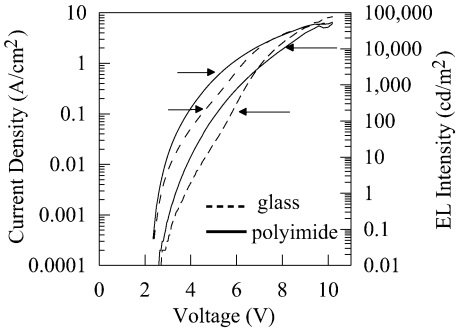

Fig. 4. Voltage–current and voltage–EL intensity characteristics of OLED fabricated on glass and polymeric substrates.

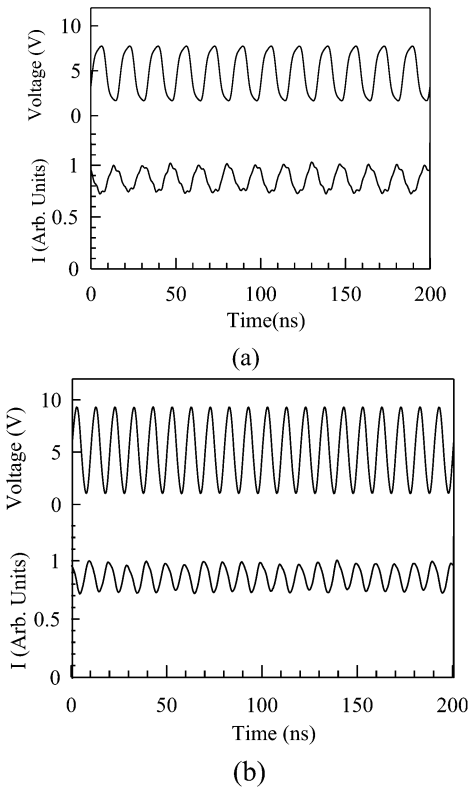

Fig. 5. Direct modulation of OLED with the emissive layer of (a) Alq3 and (b) rubrene doped in Alq3.

difference will come from the difference of the thickness and the refractive index of the substrates. The external emission intensity will depends upon them.

The modulation characteristics are shown compared with the device with Alq_3 and rubrene doped in Alq_3 as an emissive layer, which is shown in Fig. 5. The modulation characteristics of Alq_3 device is rather poor compared with that of rubrene doped device. Although the modulation characteristics at 50 MHz is shown in Fig. 5(a), the high-frequency modulation limit of the Alq_3 device is 60 MHz. It will be due the fluorescence lifetime of Alq_3, which is more than 10 ns [6], [7]. As is shown in Fig. 5(b), the OLED with rubrene doped in Alq_3 layer shows 100 MHz modulation by applying 9 V pulse voltage to the OLED, and the modulation ratio of output light is about 30%. In order to enhance the response of the OLED, it is effective to apply bias voltage to the OLED in addition to the pulsed voltage. The response of more than 100 MHz was obtained by applying lower pulsed voltage with a bias voltage. The bias voltage is selected as equivalent to the turn-on voltage of the OLED.

The OLED is fabricated directly on a polymeric waveguide, which is shown Fig. 6. Both sides of the polymeric waveguide are covered with thin film of silicone oxide (Si_2O_3) and silicone nitride (Si_3N_4) to prevent oxide and humid gases to penetrate into organic layers. Multilayer of Si_2O_3 and Si_3N_4 is effective to stick indium-tin-oxide electrode to the polymeric waveguide substrate and to prevent the harmful gas to penetrate into the organic layers. In order to improve the reflection at the 45° cut mirror, gold metal is deposited. The output light from the OLED (active area: 100 μm in square) through the transparent anode is reflected at the 45° cut, and is led to the core of the waveguide. The ITO anode was fabricated by using a mirrortron-type sputtering system (Thin-Film Process Soft Inc., Japan). Using the sputtering system, we can obtain high-quality ITO film without annealing process of the deposited film. The ITO film has a resistivity in the order of the 4×10^{-4} Ωcm. The polymeric waveguide (core size: 70 μm in square) is connected to the polymeric optical fiber (core size: 62.5 μm in diameter), and the output light from the fiber is led to the photo detectors. The OLED is consisted of an ITO-coated polymeric waveguide substrate, 50-nm-thick α-NPD as a hole transporting layer, 30-nm-thick dimethyl boryl anthracene derivative [8] as an emissive layer, 20-nm-thick 2,5-bis (2′, 2″- bipyridin—6-yl)-1,1-dimethyl-3,4-diphenyl silacyclopentadiene (PyPySPyPy) [9]–[12] as an electron transporting layer, terminated with a bilayer cathode of LiF and aluminum.

In Fig. 7(a), the emission spectrum of rubrene doped OLED is shown for a device fabricated on a glass substrate and that fabricated on a polymeric waveguide. The emission spectrum from the OLED fabricated on a glass substrate is denoted as "glass," and that from the device fabricated on a polymeric waveguide and after transmission of the polymeric waveguide is denoted as "waveguide." The device size of the yellow light-emitting LED was 0.016 mm^2. In Fig. 7(b), the typical modulation signals from the OLED fabricated on a polymeric waveguide as a substrate. The optical pulse was created by applying a 6 V pulse with a 50 MHz repetition. The response shows that we can obtain more than 50 MHz light pulse with the OLED fabricated on a polymeric waveguide for optical interconnection applications.

The proposed polymeric integrated devices can also be applicable to electrooptical conversion devices for transmitting high modulation signals in data communication systems of local-area networks (LANs), such as home networks and car LAN. Using the yellow light-emitting OLED with an active size of 0.015 mm^2 fabricated on the polymeric waveguide for generating optical pulses as electrooptical conversion processing, optical transmission experiments were demonstrated as shown in Fig. 8(a). The video and audio signals are converted to NTSC signals, and the signals are modulated by pulse frequency modulation (PFM), in which the pulse width is kept constant and the pulse generation cycle is modulated, to ensure error-free transmission. The baseband frequency of PFM signals is kept at 20 MHz. The transmission signals have a bandwidth of the video and audio signals from 50 Hz to 4.2 MHz, and 60 Hz to 10 kHz, respectively. Typical PFM signals have a carrier wave of 20±5 MHz as shown in Fig. 8(b).

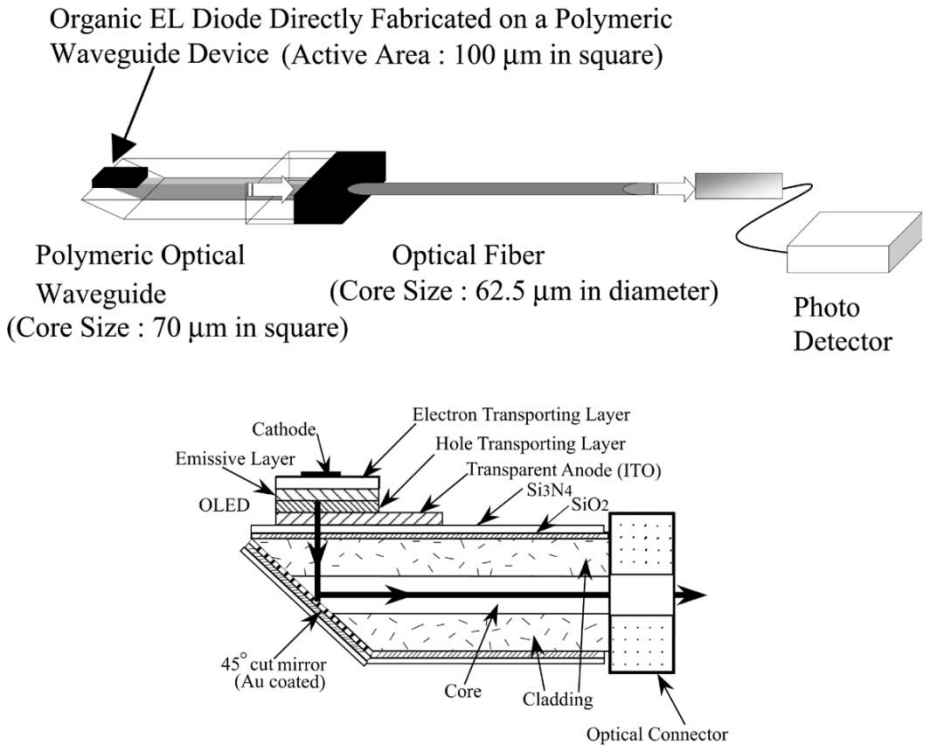

Fig. 6. Configuration of polymeric integrated devices fabricated on polymeric optical waveguide.

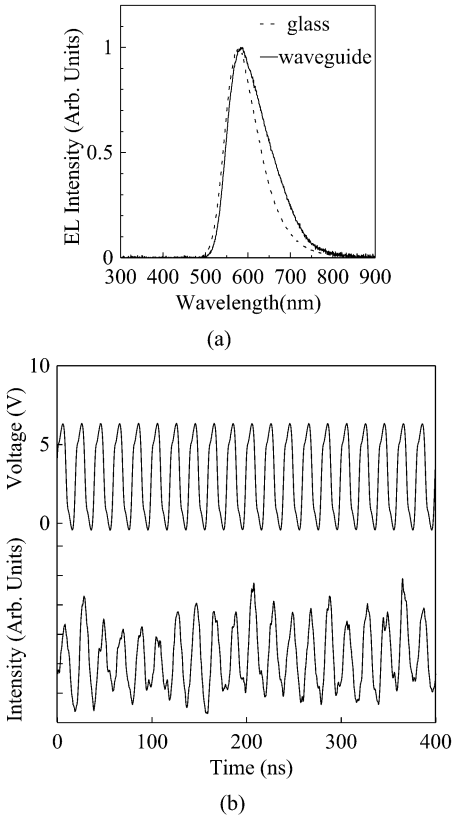

Fig. 7. Emission characteristics of OLED. (a) Emission spectra of OLED fabricated on glass and waveguide substrate. (b) Modulation signal from OLED fabricated on polymeric waveguide.

The PFM converted voltage signals are applied to the OLED. In this case, the OLED was driven by applying a low dc bias of 2.4 V. The optical signals emitting from the OLED are transmitted through polymeric waveguide with a 45° cut mirror, and through the standard multimode optical fiber with core size of 200 μm and the length of 100 m. After transmission of 100 m, the clear transmitted signals are obtained as shown in Fig. 8(b). As is shown in Fig. 8(c), the clear NTSC signals are reproduced using the optical transmission system of OLED. We can obtain clear moving picture after transmission over 100 m using the optical transmission system with he OLED. These results show that this optical integrated device, on which OLED was mounted on a polymeric waveguide, can be used as electrooptical conversion devices for optical link.

IV. Results and Discussions for OPDs

TiOPc shows the absorption band region of 950–550 nm with the peak wavelength at 729 nm and have a shoulder at 652 nm, and for F_{16}ZnPc there are the absorption band of 900–500 nm with the peaks at 645 and 810 nm. These results show that these materials have good photo sensitivity to the red LED (640 nm) used for this experiment.

In Fig. 9(a), the comparison of photo response of the OPD with five periods of multilayered TiOPc/F_{16}ZnPc devices (individual layer thickness, $d = 4$ nm) is shown. The device consisted ITO anode, five periods of multilayered TiOPc/F_{16}ZnPc as carrier generation and recombination layers, BCP as contact layer to anode and silver anode. Shown in curve (a), in Fig. 9(a), the device shows the good rectifying characteristics under dark conditions. On the other hand, under red light illumination from the LED, the device shows good photo response in the reverse bias region, as is shown in curve (b), in Fig. 9(a).

Photo-response output signals of OPDs are shown in Fig. 9(b) for five periods (individual layer thickness, $d = 4$ nm) of multilayered TiOPc/F_{16}ZnPc devices. The device is measured under

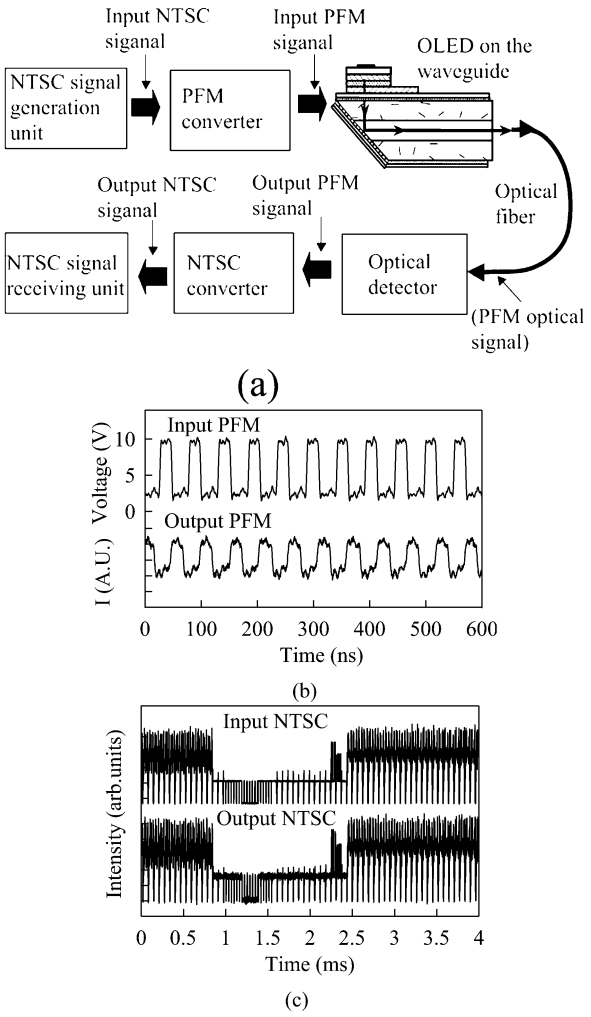

Fig. 8. Polymeric optical interconnection. (a) Configuration of optical interconnection. (b) Input and output signals of PFM signals. (c) Input and output signals of NTSC signals.

different reverse bias voltages, no bias voltage for curve (a), −2 V applied field for curve (b), and −5 V applied field for curve (c). It was found that the device has response to the light pulse at a few kilohertz of frequency without applying reverse bias voltage. The cutoff frequency of the multilayered metal-phthalocyanine hetero-junction device reached to the limit at about 6 kHz without the external reverse field. The magnitude of current density was increased with the increase of applying reverse bias voltage, and it reaches to 100 KHz with reverse voltage of 2 V, and then it reaches to 1 MHz of cutoff frequency under reverse bias voltage of 5 V. The reason why the reverse bias application enhances the high-frequency photo-response will be due to the dissociation of photo-generated excitons [13] in each interface in the multilayer structure of metal-phthalocyanine thin films, and are accelerated by applying reverse bias in the device structure. Furthermore, increased applied reverse bias decreases the dielectric relaxation time due to the decrease of stray capacitance in the multilayered structure. Also, the electric constant of the multilayered materials are field-dependent. These results enhance the photo response of the OPD in the high-electric field in the reverse bias field.

In Fig. 9(c), the photo response of multilayered OPD with different number of layers is shown, in which the photo absorption

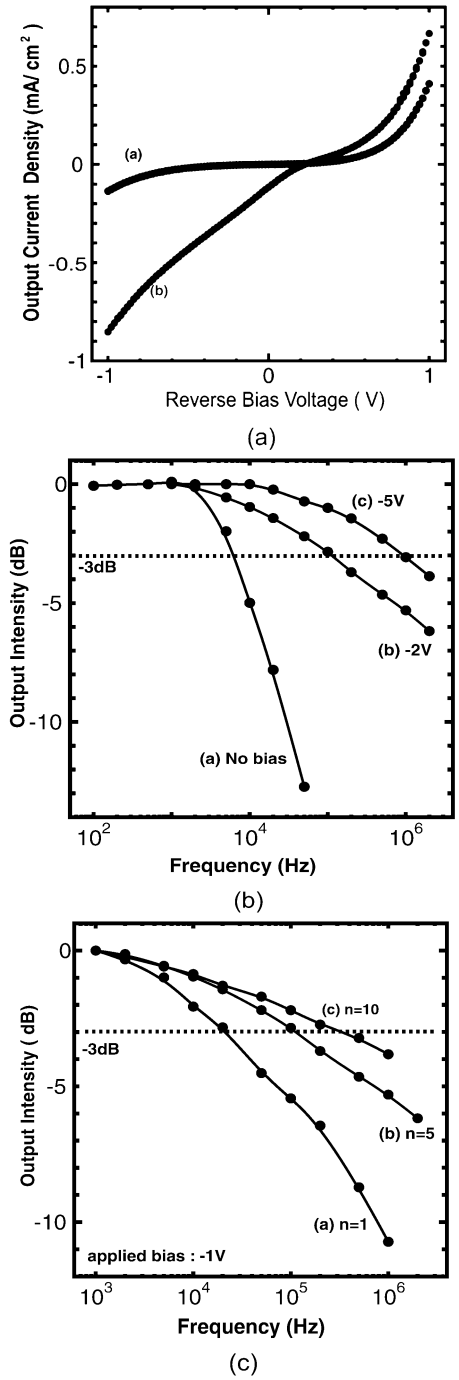

Fig. 9. Photo-response of OPD with TiOPc/F_{16}ZnPc. (a) Voltage and current characteristics of OPD curve (a): dark condition, curve (b): under red light illumination. (b) Dependence of reverse bias voltage. (c) Dependence of number of period of multilayer.

layer is kept at a constant thickness of 40 nm. The output intensity is shown in the modulation depth of the output signals in the OPD. Among them, ten periods of multilayered TiOPc/F_{16}ZnPc device [curve (c) in Fig. 9(c)] shows the remarkable increase in cutoff frequency up to more than 1 MHz. The incident photon reached to the photo-absorption layers of TiOPc and F_{16}ZnPc and the photo-generated excitons are effectively dissociated to free electrons and holes by external field applied, and then recombine in the thin-film multilayer resulting into photocurrent in the external circuits. Furthermore, the acceleration of photo-

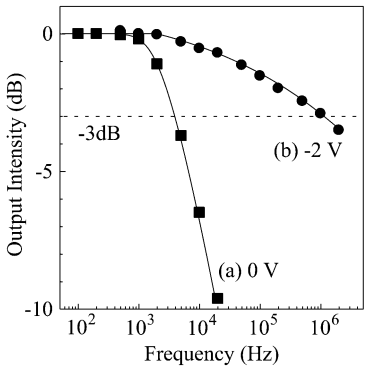

Fig. 10. Photo-response of OPD with TiOPc/F16CuPc under reverse bias conditions.

generated carriers in the thin layers by applying reverse bias voltage improves the cutoff frequency of the thin multilayered device. These results show that the cutoff frequency remarkably increases with decreasing the layer thickness under the same total layers thickness. The results will be due to fast dissociation and recombination of photo-generated carriers in thin layers with decreasing the layer thickness and increasing the numbers of interfaces of the organic layers.

In case of fluorinated cupper phthalocyanine as an n-type carrier generating layer, the frequency dependence of the output intensity is shown in Fig. 10. The device has a 4 kHz cutoff frequency under no bias field, which is shown in curve (a), in Fig. 10. On the other hand, as is shown curve (b) in Fig. 10, the cutoff frequency is improved to 1 MHz utilizing ten periods of multilayered TiOPc/F_{16}CuPc device under reverse bias of 2 V. Application of reverse bias improves the photo response by about two orders of magnitude.

In order to improve the device characteristics of the OPD, fluorinated phthalocyanine is replaced by electron conductive BPPC layers. In Fig. 11(a) and (b), photo response of the OPD with five periods of TiOPc and BPPC layers are shown for pulsed light input of 100 KHz and 1 MHz with reverse bias at 4 V, respectively. The device consisted of ITO anode, multilayer of TiOPc, and BPPC layers, where the total layer thickness was kept as 40 nm, BCP contact layer to anode, and silver anode. As is shown in Fig. 11, the OPD have good photo response under reverse bias conditions both for 100 KHz and 1 MHZ input light. In Fig. 11(c), output intensity of the OPD with five periods of TiOPc and BPPC multilayers is shown. Increasing the reverse bias condition, the photo response is increased as is the same as for the device with TiOPc and fluorinated phthalocyanine multilayers. The cutoff frequency for the device with TiOPc and BPPC multilayer increased to 5 MHz at the reverse bias condition. The reason why the device shows high performance will be due to the small leakage current. The interface between TiOPc and BPPC layers will be increased and the good quality of p-n junction was created utilizing the stack layers of TiOPc and BPPC layers.

In Fig. 12, the energy band diagram of the materials which consist of OPD is shown, where the energy levels of phthalocyanines are take from a literature [14]. The photo-generated carriers in TiOPc/F_{16}ZnPc or TiOPc/BPPC layers are transferred and accelerated by the bias field and recombine with each other. In case of TiOPc/BPPC layers, the HOMO

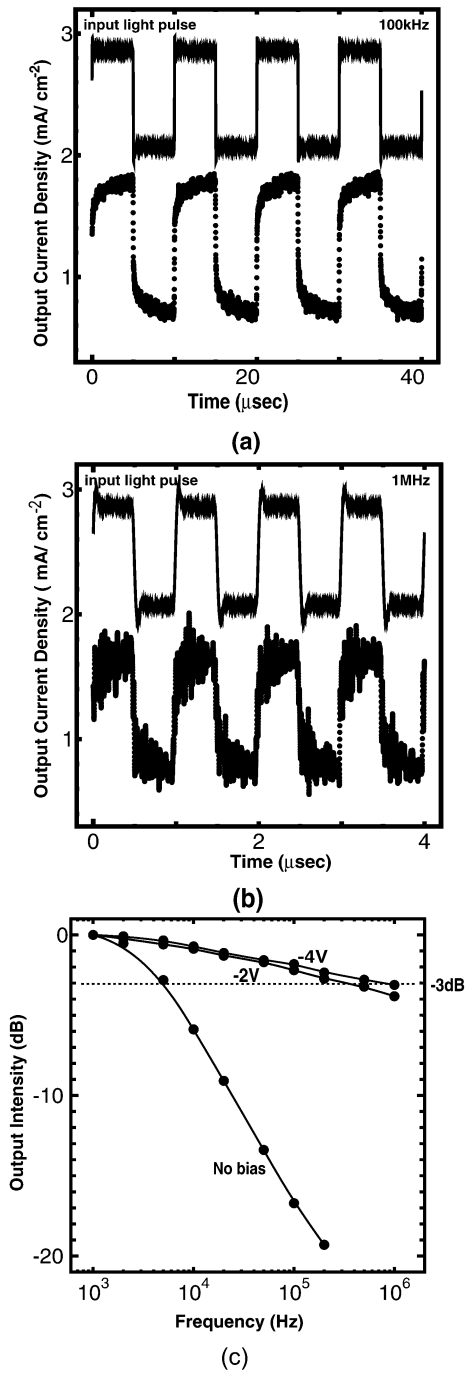

Fig. 11. Photo-response of OPD with TiOPc/BPPC. (a) 100 KHz optical pulse. (b) 1 MHz optical pulse. (c) Dependence of applied reverse voltage.

levels of TiOPc and BPPC layers are nearly the same, whereas in case of TiOPc/F_{16}ZnPc layers, that of F_{16}ZnPc layer is lower than those of TiOPc and BPPC layers. In case of photo-generated carriers in TiOPc/BPPC layers, only holes are confined in the HOMO level of TiOPc layers, whereas in the case of TiOPc/F_{16}ZnPc layers, holes and electrons are separately confined in the different layers. Namely, electrons and holes are strongly confined in the F_{16}ZnPc and TiOPc layers, respectively. As a result, leakage current decreases in the TiOPc/BPPC layers. The reason why the TiOPc/BPPC layer system decreases the leakage current is not clear at this

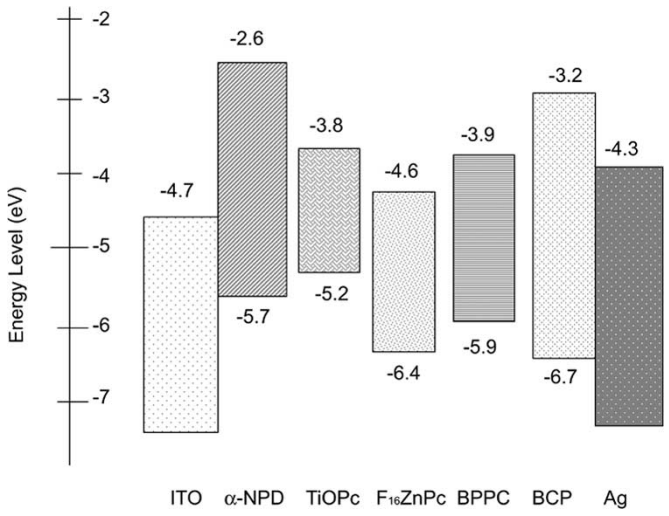

Fig. 12. Schematic of energy levels of materials used in the OPD.

stage of the experiment, however, the difference in conduction type or difference in the molecular system may result in the decrease in the leakage current.

V. Summary

In summary, an OLED was fabricated on polymeric substrate, i.e., on polymeric waveguide as a substrate. The OLED with rubrene doped in Alq_3 as an emissive layer emits more than 70 000 cd/m^2. As far as modulation frequency, the OLEDs with rubrene doped in Alq_3 and TPP doped in Alq_3 show more than 100 MHz with direct modulation of voltage pulse. However, in case of the OLED with Alq_3 as an emissive layer, the modulation frequency limited to 60 MHz due to the fluorescence lifetime of the material. We found that the fluorescence lifetime of the emissive material is one of the determinant factors for the modulation speed of OLED. The clear moving picture can be obtained through a polymeric waveguide and an optical fiber utilizing OLED as an electrooptical conversion device. We demonstrate that an OLED fabricated on a polymeric waveguide can be applicable as an electrooptical conversion device for short range optical communication. Using OLED as an electrooptical conversion device, we demonstrated a transmission of moving pictures as the initial step in fabricating flexible electrooptic devices. The OLED fabricated on a polymeric waveguide as substrate can be successfully used as a light source of electrooptic conversion device.

The pulse response of photodetectors, which consists of multilayered phthalocyanines with TiOPc and fluorinated phthalocyanine and perylene derivative (BPPC), has been discussed. As a result, reducing the individual layer thickness and applying a high voltage to the device improve the cutoff frequency of OPD, and the cutoff frequency of the device with five periods of 4-nm-thick multilayered TiOPc/BPPC hetero-structure shows more than 5 MHz at an applied bias of 4 V.

Acknowledgment

The authors would like to thank T. Fujiki, K. Takahashi, and M. Yamazaki, [Osaka University, Collaborative Research Center for Advanced Science and Technology (CRCast)] for their assistance in the experiments. They thank Dr. S. Tomaru, Dr. S. Imamura, Dr. J. Kobayashi, and Dr. F. Yamamoto (NTT Advanced Technology Corporation) for their support in the research. They also thank Dr. M. Uchida (Chisso Corporation) for providing organic materials of dimethyl boryl anthracene and silole derivatives.

References

[1] M. A. Baldo, S. Lamansky, P. E. Burrows, M. E. Thompson, and S. R. Forrest, "Very high-efficiency green organic light-emitting devices based on electrophosphorescence," *Appl. Phys. Lett.*, vol. 75, pp. 4–6, 1999.

[2] P. Peumans, V. Bulovic, and S. R. Forrest, "Efficient, high-bandwidth organic multilayer photodetectors," *Appl. Phys. Lett.*, vol. 76, pp. 3855–3857, 2000.

[3] M. Hikita, S. Tomaru, K. Enbutsu, N. Ooba, R. Yoshimura, M. Usui, T. Yoshida, and S. Imamura, "Polymeric optical waveguide films for short-distance optical interconnects," *IEEE J. Select. Topics Quantum Electron.*, vol. 5, pp. 1237–1242, Sept.-Oct. 1999.

[4] Y. Ohmori, H. Ueta, Y. Kurosaka, M. Hikita, and K. Yoshino, "Organic EL diode with plastic waveguide devices," *Nonlinear Opt.*, vol. 22, pp. 461–464, 1999.

[5] Y. Ohmori, M. Hikita, H. Kajii, T. Tsukagawa, K. Yoshino, M. Ozaki, A. Fujii, S. Tomaru, S. Imamura, H. Takenaka, J. Kobayashi, and F. Yamamoto, "Organic electroluminescent diodes as a light source for polymeric waveguides—Toward organic integrated optical devices," *Thin Sold Films*, vol. 393, pp. 267–272, 2001.

[6] C. W. Tang, S. A. Vanslyke, and C. H. Chen, "Electroluminescence of doped organic thin films," *J. Appl. Phys.*, vol. 65, pp. 3610–3616, 1989.

[7] C. Hosokawa, H. Tokailin, H. Higashi, and T. Kusumoto, "Transient behavior of organic thin film electroluminescence," *Appl. Phys. Lett.*, vol. 60, pp. 1220–1222, 1992.

[8] M. Uchida, Y. Ono, H. Yokoi, T. Nakao, and K. Furukawa, "Undoping type of highly efficient organic light emitting diodes," *J. Photopolym. Sci. Technol.*, vol. 14, pp. 305–310, 2001.

[9] K. Tamao, M. Uchida, T. Izumizawa, K. Furukawa, and S. Yamaguchi, "Silole derivatives as efficient electron transporting materials," *J. Amer. Chem. Soc.*, vol. 118, pp. 11 974–11 975, 1996.

[10] M. Uchida, T. Izumizawa, T. Nakano, S. Yamaguchi, K. Tamao, and K. Furukawa, "Structural optimization of 2,5-diarylsiloles as excellent electron-transporting materials for organic electroluminescence devices," *Chem. Mater.*, vol. 13, pp. 2680–2683, 2001.

[11] H. Murata, Z. H. Kafafi, and M. Uchida, "Efficient organic light-emitting diodes with undoped active layers based on silole derivatives," *Appl. Phys. Lett.*, vol. 80, pp. 189–191 2002.

[12] S. Tabatake, S. Naka, H. Okada, H. Onnagawa, M. Uchida, T. Nakano, and K. Furukawa, "Low operational voltage of organic electroluminescence devices with a high bipolar conducting silole derivatives," *Jpn. J. Appl. Phys.*, vol. 41, pp. 6582–6585, 2002.

[13] J. J. M. Hills, C. A. Walsh, N. C. Greenham, E. A. Marseglia, R. H. Friend, S. C. Moratti, and A. B. Holmes, "Efficient photodiodes from interpenetrating polymer networks," *Nature*, vol. 376, pp. 498–501, 1995.

[14] M. Pfeiffer, K. Leo, and N. Karl, "Fermi level determination in organic thin films by the kelvin probe method," *J. Appl. Phys.*, vol. 80, pp. 6880–6883, 1996.

Yutaka Ohmori (M'79–SM'97) was born in 1949. He received the Doctor of Engineering degree from the Department of Electrical Engineering, Faculty of Engineering, Osaka University, Osaka, Japan, in 1972.

In 1977, he joined Nippon Telegraph Telephone Public Corporation (now NTT Corporation), where he worked mainly in research on optical semiconductor devices. In 1989, he became an Associate Professor in the Department of Electronic Engineering, Faculty of Engineering, Osaka University. In 2000, he became a Professor in the Collaborative Research Center for Advanced Science and Technology (CRCast), Electronic Materials and Systems Engineering, Osaka University, where he worked on optical and electrical devices utilizing organic materials including conducting polymers.

Dr. Ohmori is a Member of the Institute of Electronics, Information, and Communication Engineers, the Japan Society of Applied Physics, the American Physical Society, and the Materials Research Society.

Hirotake Kajii was born in Kobe, Japan, in 1974. He received the B.S., M.S., and Ph.D. degrees in electronic engineering from the Faculty of Engineering, Osaka University, Osaka, Japan in 1996, 1998, and 2000, respectively.

In 2000, he joined the Collaborative Research Center for Advanced Science and Technology, Osaka University, where he is currently a Research Associate. His research interests are in the electronic and optical properties of organic materials, and application of them to electronic devices such as photocell and LED.

Dr. Kajii is a Member of the Institute of Electronics, Information, and Communication Engineers, the Institute of Electrical Engineers of Japan, and the Japan Society of Applied Physics.

Masamitsu Kaneko was born in 1971. He received the Doctor of Information Science degree from the Department of Computer Science and Electronics, Faculty of Computer Science and Systems Engineering, Kyushu Institute of Technology, Fukuoka, Japan, in 1995.

In 1999, he joined Fukuoka Industry, Science and Technology Foundation, where he worked mainly in research on organic photovoltaic cells. In 2002, he became a Postdoctoral Researcher in the Collaborative Research Center for Advanced Science and Technology, Osaka University, Osaka, Japan, where he worked mainly in research on optical and electrical devices using organic materials.

Dr. Kaneko is a Member of the Institute of Electronics, Information, and Communication Engineers in Japan and the Japan Society of Applied Physics.

Katsumi Yoshino (SM'97–F'04) was born in Shimane, Japan, on December 10, 1941. He graduated in 1964 from the Department of Electrical Engineering, Faculty of Engineering, Osaka University, Osaka, Japan, where he received the Doctor of Engineering degree in 1969.

In 1969, he became a Research Associate in electrical engineering, Osaka University. He became an Associate Professor in 1972. In 1988, he became a Professor of electronic engineering at the Faculty of Engineering, Osaka University. He has been engaged in research on organic functional materials such as conducting polymers, optical functional polymers, and ferroelectric liquid crystals. He authored or coauthored more than 30 books.

Dr. Yoshino received an Applied Physical Society Award and the Osaka Scientific Award in 1981 and 1990 and the Institute of Electrical Engineers of Japan Award in 1997 and 1998, respectively. He is a Member of the Institute of Electrical Engineers of Japan, the Japan Society of Applied Physics, the Physical Society of Japan, the Institute of Electronics, Information, and Communication Engineers, Polymer Society and Laser Society, Japan Material Society, and the American Physical Society.

Masanori Ozaki was born in Aichi, Japan, in February 1960. He graduated in 1983 from the Department of Electrical Engineering, Faculty of Engineering, Osaka University, Osaka, Japan, where he received the Doctor of Engineering degree in 1988.

He joined the Graduate School of Engineering, Electronic Engineering, Osaka University, where he is an Associate Professor. He has been engaged in research on liquid crystals, optical functional polymers, and photonic crystals.

Dr. Ozaki is a Member of the Institute of Electrical Engineers of Japan, the Japan Society of Applied Physics, the Physical Society of Japan, the Japanese Liquid Crystal Society, and the Institute of Electronics, Information, and Communication Engineers.

Akihiko Fujii was born in Osaka, Japan, on December 3, 1969. He graduated in 1993 from the Department of Electronic Engineering, Faculty of Engineering, Osaka University, Osaka, Japan, where he received the Doctor of Engineering degree in 1997.

He was a Research Fellow with the Japan Society for the Promotion of Science between 1997 and 1998. In 1998, he joined the Graduate School of Engineering, Electronic Engineering, Osaka University, where he was a Research Associate. He has been engaged in research on optical and electrical devices utilizing organic materials including dye molecules and conducting polymers.

Dr. Fujii is a Member of the Institute of Electrical Engineers of Japan, the Japan Society of Applied Physics, the Physical Society of Japan, and the Society of Polymer Science, Japan.

Makoto Hikita was born in Tokyo, Japan, in 1950. He received the B.E. and M.E. degrees in instrumentation engineering from Keio University, in 1973 and 1975, respectively, and the Ph.D. degree in physics from Osaka University, Osaka, Japan, in 1990.

In 1975, he joined NTT Musashino Laboratories and NTT Ibaraki Laboratories, Ibaraki, Japan, where he was engaged in research on superconducting telecommunication cables, superconducting materials, Josephson devices, Anderson Localization, and superconducting physics. From 1992, he has been engaged in the development of electrooptic and passive polymer optical component devices. In 2000, he joined NTT Advanced Technology Corporation (NTT-AT), Ibaraki, Japan. He is presently a Senior Engineer at NTT-AT.

Dr. Hikita is a Member of the Institute of Electronics, Information, and Communication Engineers in Japan, the Physical Society of Japan, the Japan Society of Applied Physics, and the Japan Institute of Electronics Packaging.

Hisataka Takenaka was born in 1950. He received the B.Sc., and M.Sc. degrees in physics, and the D.Sc. degree from Kwansei Gakuin University, Hyogo, Japan, in 1974, 1976, and 1979, respectively.

In 1979, he joined Nippon Telegraph Telephone Public Corporation (now NTT Corporation), where he was engaged in the development of Josephson junctions, multilayered X-ray mirrors, and EUV lithography. He also joined NTT Advanced Technology Corporation (NTT-AT), Ibaraki, Japan, in 1996. He was a Visiting Professor in the Materials and Structures Laboratory, Tokyo Institute of Technology, in 1999. His current interests are the development of X-ray focusing optics using multilayered structure for X-ray photoemission spectroscopy and of standard samples for secondary ion mass spectrometry.

Dr. Takenaka is a Member of the Physical Society of Japan, the Japan Society of Applied Physics, and the Japan Society for synchrotron radiation research.

Takayuki Taneda graduated in 2001 from the Department of Electrical Engineering, Faculty of Engineering, Osaka University, Osaka, Japan, where he received the M.S. degree in 2003.

In 2003, he joined Sony Corporation.